17th World Conference on Earthquake Engineering, 17WCEE
Sendai, Japan - September 13th to 18th 2020

COLUMN-FOUNDATION MOMENT CONNECTIONS WITH HEADED ANCHORS: EXPERIMENTAL TESTS AND ANALYTICAL SIMULATIONS

B. Worsfold[(1)], J. Moehle[(2)]

[(1)] *PhD Candidate, UC Berkeley, benjamin_worsfold@berkeley.edu*
[(2)] *Ed and Diane Wilson Presidential Professor of Structural Engineering, UC Berkeley, moehle@berkeley.edu*

Abstract

Steel and precast columns are commonly designed to transfer moment loads to concrete foundations through cast-in-place headed anchors. In the United States, three different design methods have been used to design these connections:

1. Anchoring-to-concrete provisions (e.g., ACI 318-14 Chapter 17);
2. The strut-and-tie method (e.g., ACI 318-14 Chapter 23); and
3. Joint shear design methods (e.g., ACI 352R-02).

For any given connection, the strengths calculated with these three methods can differ by a wide margin.

A laboratory test was performed to provide benchmark physical data to determine the applicability of the three aforementioned design methods. The test specimen consisted of a full-scale interior column-foundation connection located away from footing edges. The specimen was tested until failure under cyclic quasi-static loading. No axial load was applied to the column in order to isolate the effects of moment loading. Practicing engineers contributed to the design of the test specimen so the geometry and materials would closely resemble elements of current construction practice on the West Coast of the United States. Analytical finite element models were calibrated with the experimental data and sensitivity studies were performed.

Experimental and analytical results suggest that the anchoring-to-concrete provisions from the US concrete building code (ACI 318-14 Chapter 17) are an appropriate method for the design of column-foundation connections with cast-in-place headed anchors governed by moment transfer. Alternative methods can be unconservative. This paper documents the various design methods, the test specimens, analytical models, and the design implications of the tests.

Keywords: column-foundation connections; anchoring to concrete; breakout; beam-column joints; strut-and-tie

1. Introduction

A lack of consensus exists in the structural engineering community as to what methods are most appropriate for the design of steel-column-to-concrete-foundation connections with headed anchors. For connections governed by moment transfer, three different design methods have been used in practice in the United States:

1. Anchoring-to-concrete provisions considering concrete breakout (e.g., ACI 318-14 Chapter 17 [1]);
2. The strut-and-tie method (e.g., ACI 318-14 Chapter 23); and
3. Joint shear design methods (e.g., ACI 352R-02)

The strengths calculated by these three methods can differ by a wide margin. Some practicing engineers gravitate towards the latter two methods as designs based on concrete breakout equations can be conservative and costly. Some proponents of strut-and-tie modeling contend that a properly designed footing will have internal force-resisting mechanisms that can be arranged naturally to resist the internal forces associated with anchoring the anchor bolts, thereby avoiding breakout failure. A counter argument is that if breakout capacities are reached, breakout failure will occur regardless.

A laboratory test was performed to provide benchmark physical data by which to determine the applicability of these aforementioned design methods. Practicing engineers were consulted so the geometry and materials of the test specimens would closely resemble elements of current construction practice on the West Coast of the United States.

2. Current Design Methodologies

2.1. Concrete Breakout Equations

The tensile force in cast-in-place headed anchors is transferred to the concrete at the bearing surface of the heads, causing local tensile stresses. When the tensile capacity of concrete is exceeded, cracks initiate around the anchor heads and propagate towards the surface in a radially symmetric pattern, detaching a cone-shaped volume of concrete. This failure mode, known as concrete breakout, is easily identifiable due to the cone-shaped segment of detached concrete.

ACI 318-14 Chapter 17 breakout equations are based on linear elastic fracture mechanics and the concrete capacity design (CCD) approach by Fuchs, 1995 [2]. This method assumes a 35° cone as shown in Fig. 1 and a uniform tensile stress along the failure surface, which results in the following equation for basic concrete breakout strength of a single anchor under tension in cracked concrete:

$$N_b = k_c \sqrt{f_c'}\, h_{ef}^{\alpha} \tag{1}$$

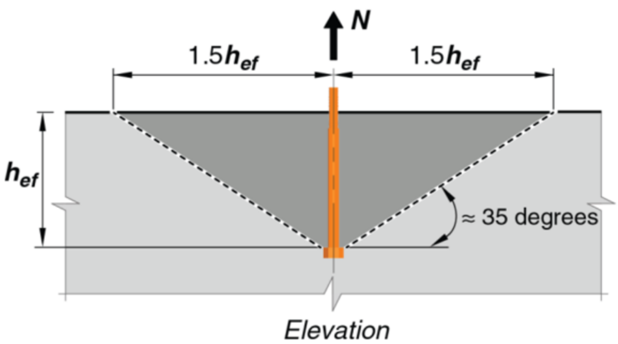

Fig. 1 – Assumed geometry of concrete breakout cone for ACI breakout equations (ACI Committee 318, 2019).

To calculate the capacity of an anchor group, the basic concrete breakout strength is multiplied by five modification factors to account for group effects, load eccentricity, edge distance, uncracked concrete, and concrete splitting respectively with the following equation:

$$N_{cbg} = \frac{A_{Nc}}{A_{Nco}} \, \Psi_{ec,N} \, \Psi_{ed,N} \, \Psi_{c,N} \, \Psi_{cp,N} \, N_b \quad (2)$$

Numerical simulations and experimental testing have shown that Eq. (2) can be conservative where moment transfer results in flexural compression applied to the concrete surface close to the anchors that are in tension ([3] and [4]). The bearing of the base plate on the surface of the potential concrete breakout cone may delay the formation of this failure mechanism. To account for this effect, various researchers have proposed modification factors [2]. As an example, Herzog (2015) [3] proposes the following modification factor that should multiply Eq. (2):

$$\Psi_M = 2.5 - z/h_{ef} \ \geq 1.0 \quad (3)$$

The joint aspect ratio (z/h_{ef}), where z is the perpendicular distance between the flexural tension and flexural compression resultants, serves as a proxy to determine if the compressive bearing force is acting on the cone surface or if it is too far away to have a significant effect. This factor is not included in ACI 318-14, but a similar version can be found in Eurocode 2 - Part 4 [15].

2.2. Strut-and-Tie Method

The strut-and-tie method was developed for the design of regions near geometric discontinuities or points of load application where the assumptions of traditional beam theory do not apply. A strut-and-tie model is created by devising a truss-type structure inside a reinforced concrete member that transfers loads from the point of application to the supports through elements that carry either uniaxial compressive forces (struts) or uniaxial tensile forces (ties). The regions where struts and ties intersect are known as nodes. Failure occurs when either 1) a strut fails by crushing or by splitting longitudinally, 2) a tie yields, or 3) a node fails to transfer the loads among the elements that frame into it. ACI 318-14 Chapter 23 describes this method limiting the usable capacity of each element.

2.3. Beam-Column Joint Design

Joint committee ACI-ASCE 352 [5] provides recommendations for the proportioning, design, and reinforcing details of concrete beam-column joints. The horizontal joint shear capacity depends on the concrete compressive strength and the joint geometry as shown below:

$$V_n = \gamma\sqrt{f_c'}\, b_j h_c \quad (4)$$

where γ is defined by the joint geometry, f_c' is the concrete compressive strength, and the product $b_j h_c$defines the effective joint area.

The geometry and force flow of a column-foundation connection with headed anchors resembles that of a roof joint where the column reinforcement terminates in headed rebar. Due to the similarities in geometry and force flow, it has been suggested, that the horizontal-joint-shear method should be applicable to the design of column-foundation connections with headed anchors.

The commentary of ACI 318-14 suggests that if z/h_{ef} is less than about 1.4, then breakout is precluded and it is not required to check for breakout failure using Chapter 17 of ACI 318.

3. Physical Testing

3.1 Test specimen

The test specimen shown in Fig. 2 is a full-scale interior column-foundation connection with headed anchors. No axial load is applied to the column to isolate the effect of moment loading. The specimen is loaded cyclically and quasi-statically with a displacement driven loading protocol in the strong direction of the steel column. To simplify the test setup without critically compromising the test purposes, the slab is simply supported at its ends rather than being supported on a soil-like medium.

The column consisted of an A992 Grade 50 [345 MPa] W12 x 112 steel section (see Fig. 2). The column was welded to a 24 in. by 21.5 in. by 2-3/4 in. [610 mm by 546 mm by 70 mm] A529 Grade 50 [345 MPa] steel base plate with a 5.25 in. by 5.25 in. by 2 in. [133 mm by 133 mm by 51 mm] A529 Grade 50 [345 MPa] shear lug. The base plate and shear lug were grouted in place to the concrete foundation. Four 1-1/2 in. [38 mm] diameter Grade 105 [725 MPa] anchor bolts with heavy hex nuts as heads were cast in place on each side of the column at an effective embedment depth of 14.3 in. [363 mm]. Each anchor was prestressed to a torque of 120 lb-ft [163 N-m].

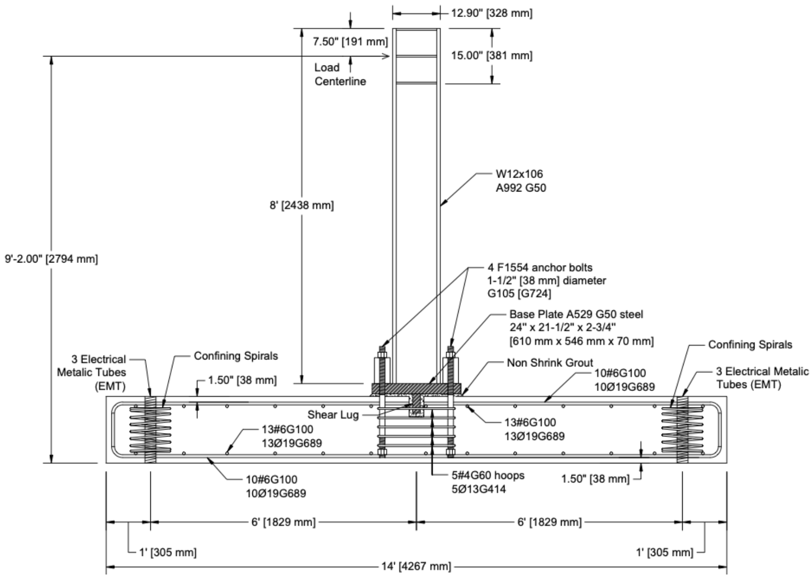

Fig. 2 – Elevation view of test specimen longitudinal cross section.

The 18 in. [457 mm] thick foundation slab is designed such that it has sufficient shear and moment strength to resist the expected loading. Longitudinal reinforcement is designed assuming the reinforcement is Grade 60 [414 MPa]. However, to ensure that extensive flexural yielding does not occur if the moment transfer strength is underestimated, the provided bars are Grade 100 [725 MPa]. Longitudinal and transverse reinforcement is provided at both the top and bottom surfaces of the slab. The concrete for the foundation slab is a 4000 psi [27.6 MPa] mixture at 28 days with ¾ in. [19 mm] aggregate. Table 1 shows the tested concrete properties of the foundation slab on test day which was 21 days from casting.

Table 1 – Concrete properties of foundation slab.

f'_c psi [MPa]	3700 [25.5]
E ksi [GPa]	3470 [23.9]
f_t psi [MPa]	380 [2.62]
G_f lb/in [N/m]	0.310 [54.3]
LA Abrasion Test ¾ in. [19 mm] aggregate	21%

The joint was confined by 5#4 [ϕ13] Grade 60 [414 MPa] hoops. The hoops provided are consistent with the requirement of ACI 352 for beam-column joint confining, as well as requirements for distributed strut reinforcement in the ACI 318-14 strut-and-tie method.

3.2 Physical Specimen Results

Clear concrete breakout failure cones are observed as the peak load is reached. Two intersecting breakout cones formed, one for each anchor group for loading in opposite directions. The cones are observed to be asymmetric with a much steeper slope towards the interior of the joint. Minimum cracking and damage were observed on the bottom surface of the foundation slab. Punching of the anchors through the bottom of the slab is not observed.

The force versus drift ratio relationship of the column free end, shown in Fig. 3a, highlights the instant of failure for both the east and west anchor groups as well as the ends of pauses during loading. After breakout failure occurs, the connection resistance drops to about 50% of the maximum resistance.

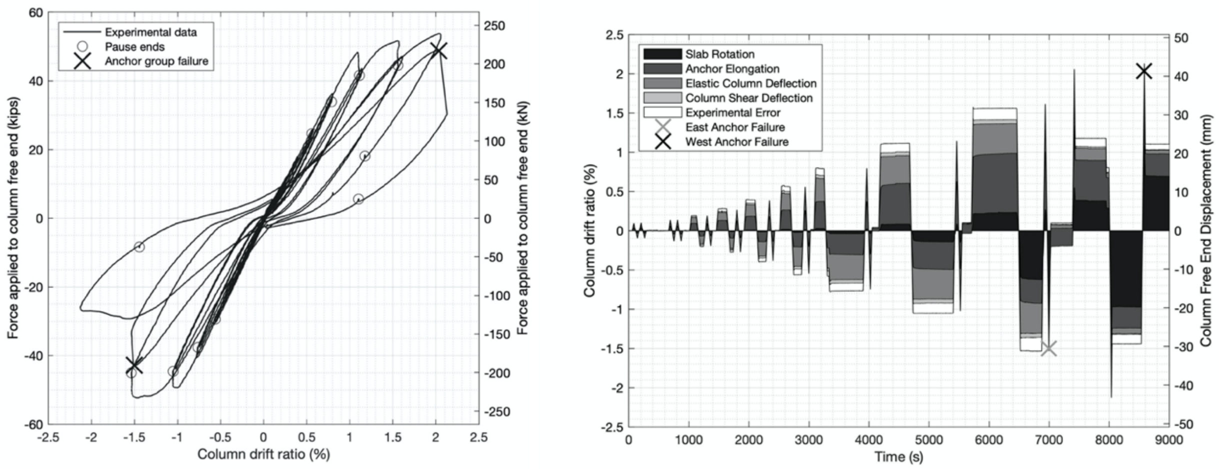

Fig. 3 – a) Force versus drift ratio relationship of the column free end moment transfer specimen and b) column drift ratio versus time divided into contributions from the slab rotation, the relative base plate rotation, the elastic column deflection, the column shear deflection, and experimental error.

Fig. 3b plots the column drift ratio versus time and subdivides the displacement into the contributions from the slab rotation, the relative base plate rotation, the elastic column deflection, the column shear deflection, and experimental error. Initially, the majority of the displacement is due to the elastic deformation of the column and anchor extension. As concrete damage progresses, the contribution of the slab rotation increases while the contribution of the elastic column decreases. For a more detailed description of the test specimen or the experimental results please refer to the report [6].

3.3 Discussion

The test specimen clearly failed in a concrete breakout mode. The cone surface that extended away from the column from the anchor heads intersected the top surface at a distance of about 1.5 to 2.0 times h_{ef}. The cone surface within the joint extended from the anchor heads toward the flexural compression zone of the steel wide-flange column. Concrete joint material was not crushed and hoops indicated little evidence of joint dilation, suggesting that beam-column joint failure did not contribute to the overall failure mechanism. There was also no evidence of crushing of struts or nodes of the intended strut-and-tie model, suggesting that strut-and-tie failure also did not contribute to the overall failure mechanism.

Consistent with the observed failure mode, the failure load obtained from the breakout equations is the closest to the experimental failure load (see Fig. 4). Including the modification factor Ψ_M, as proposed by Herzog (2015) [3], improves the results. The breakout cones are observed to be asymmetric with a much steeper slope towards the interior of the joint. This observation is consistent with Herzog (2015) [3] in that the base plate bearing pressure impedes the formation of a full breakout cone. After the maximum load is reached, the slab rotation increases significantly showing that the concrete cones have formed and are displacing essentially as rigid objects (see Fig. 3b).

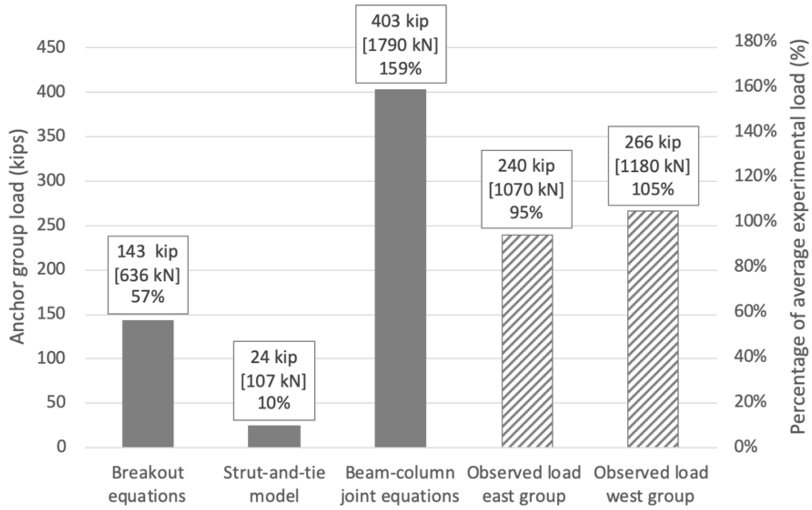

Fig. 4 – Failure loads in the anchor group according to different design methods and the experimentally observed failure loads. Note: All safety factors removed. $\phi = 1$. Also, the breakout calculations were multiplied by a factor of $f_{mean} = 1.33$ to bring the result from a 5-percentile value to a mean value.

The ACI strut-and-tie model significantly underestimates the connection strength. This may be because the ACI strut-and-tie models ignore the tension capacity of concrete which is a significant player in anchor capacity and behavior. The strut-and-tie model used could be improved if the anchor heads extended past the bottom reinforcing bars, so as to place the bottom strut-and-tie node at the same height as the bottom reinforcing bars. This way the load could follow a more direct path to the bottom reinforcing bars bypassing the hoops which are the weakest link of the current model. The slab would have to be thickened in this zone to accommodate the deeper anchors.

The horizontal-joint-shear equations overestimate the capacity of the connection. This method assumes beams with shear reinforcement frame into the joint. Even though the test specimen joint is confined on all sides by concrete slab material, the lack of shear reinforcement in this region could account for the lower than expected strength. Slab shear reinforcement could improve the connection strength.

Assuming uniform bearing pressure between the base plate and the concrete, as suggested by AISC Design Guide 1 [7], results in a joint aspect ratio z/h_{ef} of 1.3. Even though the anchors were arranged such that $z/h_{ef} \leq 1.4$, breakout failure was not avoided as suggested by the commentary in ACI 318-14 section R25.4.4.2c

In design, breakout type failures are generally avoided because they are assumed to be brittle, but Fig. 3 shows that the connection demonstrates some ductility. Also, after breakout failure, the moment capacity of the connection drops to about 50% of the maximum strength. The residual strength is higher than expected for this failure type. The top surface reinforcing bars that cross the concrete cones and the confining hoops may be responsible for preventing a more significant drop in strength.

The confining hoops placed near the top of the joint are more effective than those placed towards the bottom of the joint as the top hoops were observed to be more highly strained. Also, only the legs of the hoops that cross the concrete cone failure planes show any significant strain which is consistent with the breakout failure mechanism.

4. Finite Element Modeling

In order to better understand the failure mechanism observed during the physical test, a finite element (FE) model of the specimen was created and calibrated to fit the observed data. Sensitivity studies were performed on this model to ensure stable behavior. This robust model may then be used in the future to perform parametric studies.

4.1 Modeling approach

For this investigation, the FE software ATENA was used as it has shown good correspondence with physical test results of reinforced concrete specimens in the past [8]. Due to symmetry, only half of the specimen is required (see Fig. 5).

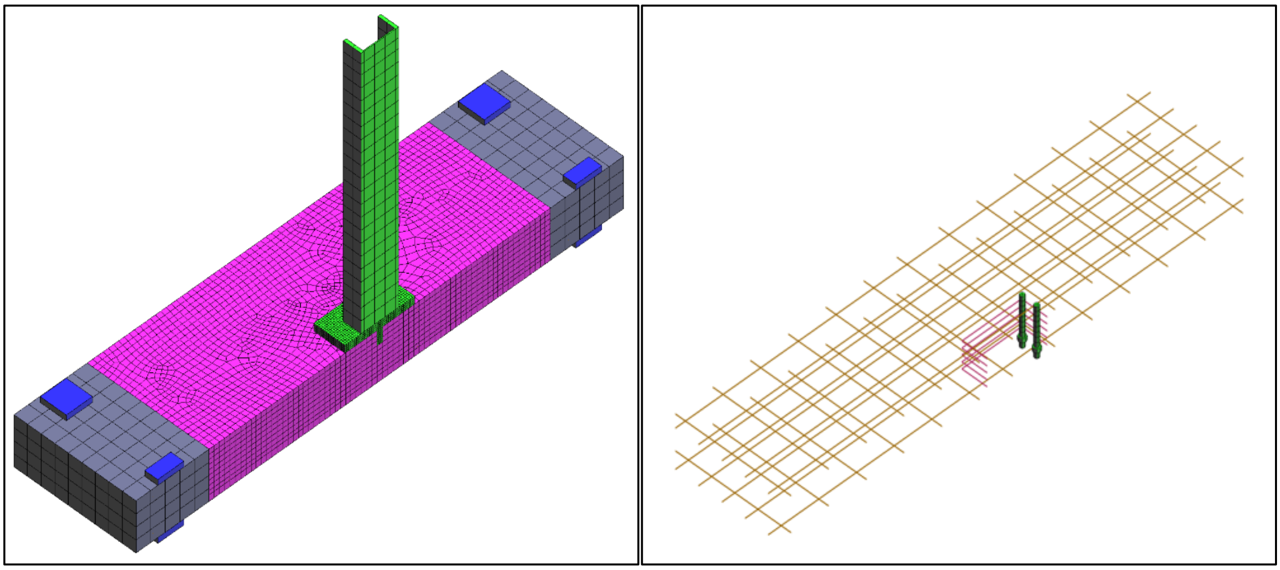

Fig. 5 – FE model of column-foundation connection showing a) materials and meshing and b) placement of anchors and reinforcing bars

The concrete is modeled with three-dimensional, 8-node hexahedra elements and a 2x2 integration scheme. The concrete material model used by ATENA is based on the smeared crack approach and uses the combined fracture-plastic model proposed by Červenka and Pappanikolaou [9]. For compressive behavior this model uses the Menetrey-William [9] relations. For tensile behavior, the concrete is elastic up until the maximum tensile capacity (f_t) is reached in the maximum principal direction (Rankine criterion). The post-peak stress-softening curve uses the crack band approach of Bažant and Oh [10] and follows the exponential crack opening curve from Hordijk [11] shown in Fig. 6. In this model, as the crack width (w_t) increases from zero to the maximum value (w_{tc}), the stress drops exponentially from the maximum tensile stress (f_t) to zero. The area under this curve is known as fracture energy (G_f). This parameter describes how much energy is required to completely open a crack such that no normal stress travels across it. The crack band width (L_t) is measured in each element perpendicular to the crack as shown in Fig. 6 and then modified as proposed by Červenka et al. [12] in Eq. (5) to account for strain localization, mesh size, and crack orientation. The crack angle (θ) is taken as the average angle between the crack and the sides of the element.

$$L_t' = \gamma L_t$$

$$\gamma = 1 + (\gamma_{max} - 1)\frac{\theta}{45} \qquad (5)$$

$$\text{with } \theta \in 0, 45 \text{ and } \gamma_{max} = 1.5$$

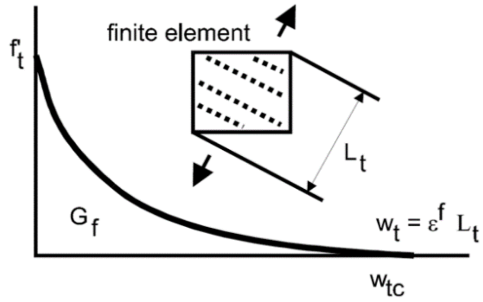

Fig. 6 – Exponential crack-opening law from Hordijk [11]

The reinforcing bars are composed of one-dimensional elements with a stress-strain curve obtained through physical testing. The anchors are modeled as three-dimensional elastic steel elements fixed to the bottom of the base plate and to the concrete along the bearing surface. The anchors are not expected to yield.

The solution algorithm uses a tangent stiffness predictor with a minimum of 140 load steps to the peak. A maximum of 120 iterations are allowed per load step with an error tolerance of 0.001.

4.2 Base Model Calibration

Three FE models of different mesh sizes (2.8 in. [71 mm], 2.3 in. [58 mm], and 1.8 in. [46 mm]) were calibrated to fit the experimental data. The models were loaded monotonically with displacements applied at the column free end. The monotonic behavior is expected to behave as an envelope for the cyclic experimental data. Fig. 7 shows the post-peak crack patterns along the specimen longitudinal cross section. Asymmetric breakout cones are observed in both models consistent with the experimental observations. The cracks originate at the anchor head and spread towards the top surface as expected. Fig. 8 shows the force to drift ratio curve for the analytical models and the experimental data. The initial stiffness of the models matches the experimental stiffness, considering the inherent uncertainty and limitations of the methods used. The experimental anchor peak loads are within the spread of the analytical peak loads. The main concrete material properties are shown in Table 2.

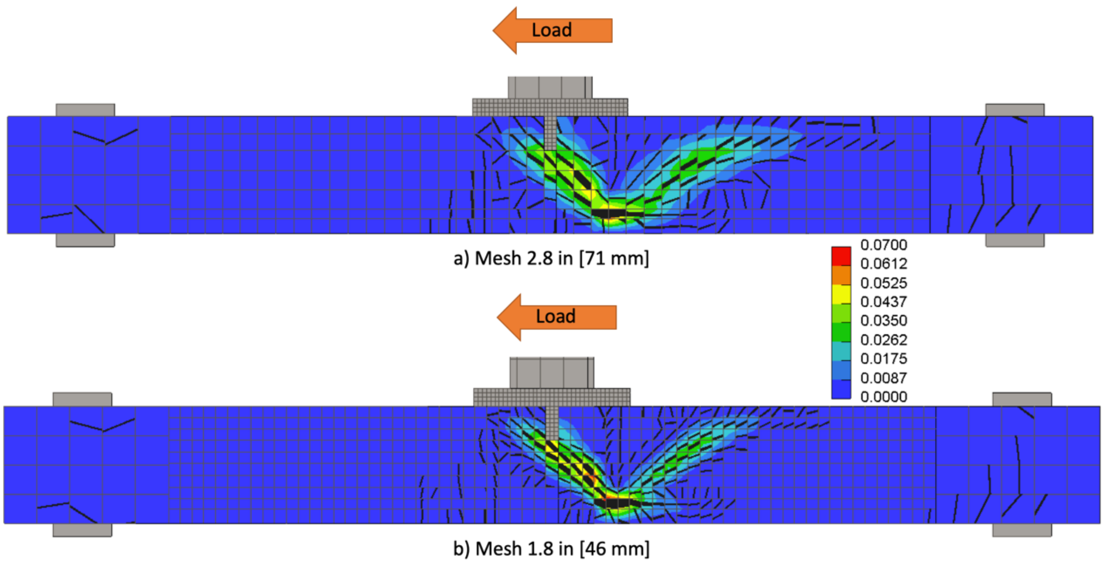

Fig. 7 – Post-peak crack patterns and maximum principal fracture strains of base model longitudinal cross section for different mesh sizes

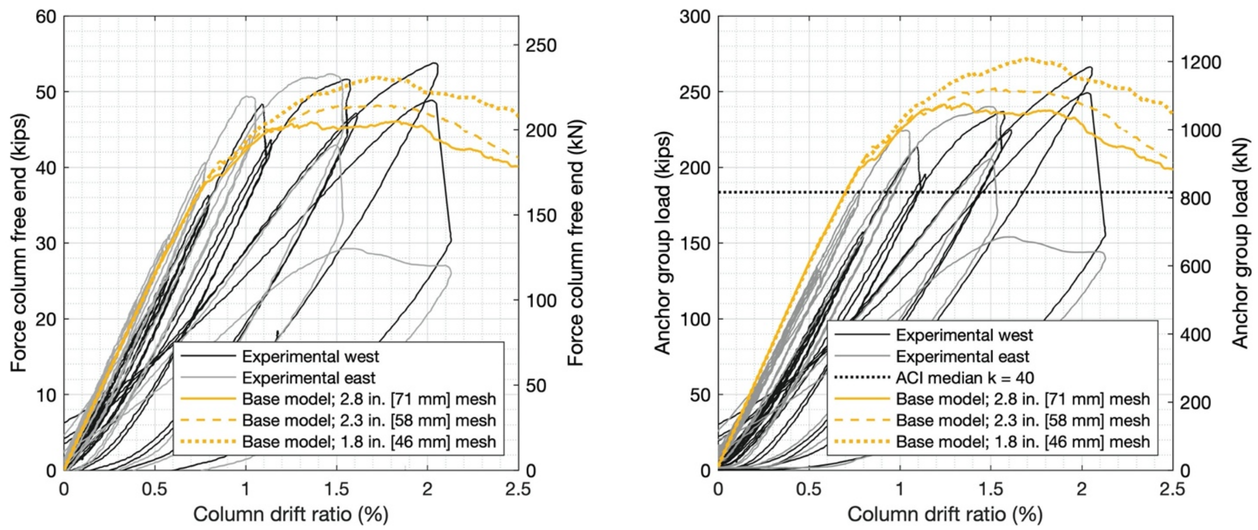

Fig. 8 –Experimental data and calibrated FE models for a) column force versus drift ratio and b) anchor group force versus drift ratio for different mesh sizes

Table 2 – Main concrete material properties of FE base models

Concrete Material Property	**Value**
Compressive strength (f'_c)	25.5 MPa [3700 psi]
Modulus of elasticity (E)	23.9 GPa [3470 ksi]
Fracture energy (G_f)	68 N/m [0.388 lb/in]
Tensile strength (f_t)	2.62 MPa [380 psi]
Dilation factor (β)	+ 0.25
Maximum aggregate size (t_{max})	19 mm [0.75 in]
Minimum crack spacing	48 mm [1.88 in]
Maximum crack spacing	203 mm [8 in]
Fixed crack	0.8

4.3 Sensitivity studies

Sensitivity studies were run to test the robustness of the previously described base models.

4.3.1 Anchor model

In the base models, the headed anchors are 3D elements with the bearing surface fixed to the concrete elements. Simpler 1D truss models were tested but, in general, show high sensitivity to mesh size and material properties when compared to 3D models. Also, 1D truss models tend to have lower convergence rates than 3D models due to bond considerations along the anchor shaft. Even though 3D models are more complex to build, they were found to be more suitable in terms of numerical stability and sensitivity to material properties for the problem at hand.

The contact between the 3D steel anchor and the concrete was initially thought to be an important parameter. Single anchor models were run with 1) interface layers between every anchor-concrete surface which allow for relative sliding, 2) interface layers along the anchor head only, 3) and a perfectly fixed contact between the anchor and the concrete along bearing surface. Fig. 9a shows the load displacement curves for these models for two mesh sizes. No significant trend is observed and all peak loads are within 5% of each other. The 3D anchor models are not particularly sensitive to the complexity of the steel-concrete interface. A fixed contact along the anchor bearing surface was selected for the base models as it seems to be sufficiently accurate and is the most numerically stable of the options considered.

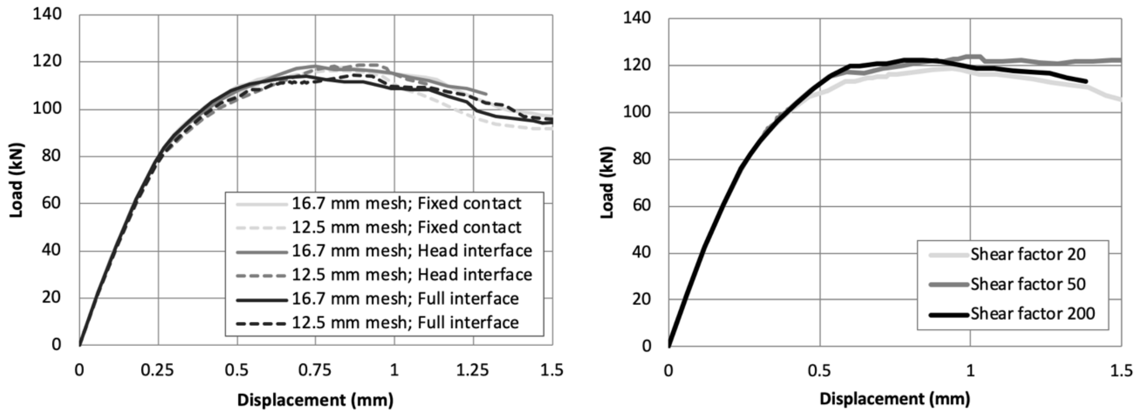

Fig. 9 – Force-displacement graphs for single 3D anchor test with a) different types of interfaces for two mesh sizes and b) different shear factors

4.3.2 Shear factor (s_f)

In the concrete material model, the shear factor (s_f) determines the shear stiffness along a cracked surface. The instantaneous stiffness perpendicular to the crack is multiplied by the shear factor to obtain the stiffness along a cracked surface. This parameter has shown to have a significant effect when modeling shear failure modes [13]. Anchor breakout problems are not expected to be sensitive to this parameter as the shear carried across the crack surface is not expected to be significant [14]. Fig. 9b shows that, as expected, single anchor breakout problems are not sensitive to this parameter as no trend is observed.

4.3.3 Mesh size

Some mesh sensitivity is expected. As the mesh changes, the exact path of the breakout cone varies which inevitably causes variations in the results. Also, as the mesh is refined the cracks concentrate into smaller regions as observed in Fig. 7. Mesh sizes corresponding to $h_{ef}/5$ to $h_{ef}/8$ were found to produce results that matched the spread of experimental results. As can be seen in Fig. 8, finer meshes tend to increase the peak load. The initial stiffness was not found to be sensitive to mesh size.

4.3.4 Base plate-concrete interface

While loading the physical specimen, some portions of the base plate would lift up off the concrete surface, while other portions would bear down against it. This behavior can be modeled analytically either with a sliding interface layer or a fixed contact in the region of bearing pressure. The sliding interface model produced an initial stiffness closer to the experimental observations as can be observed in Fig. 10. Also, the sliding interface model converged more quickly and with lower errors than the fixed model. To produce reasonable results, the interface layer was applied to the bearing surface of the base plate and shear lug. The sliding interface contact was selected for the base models due to the higher numerical stability and better initial stiffness.

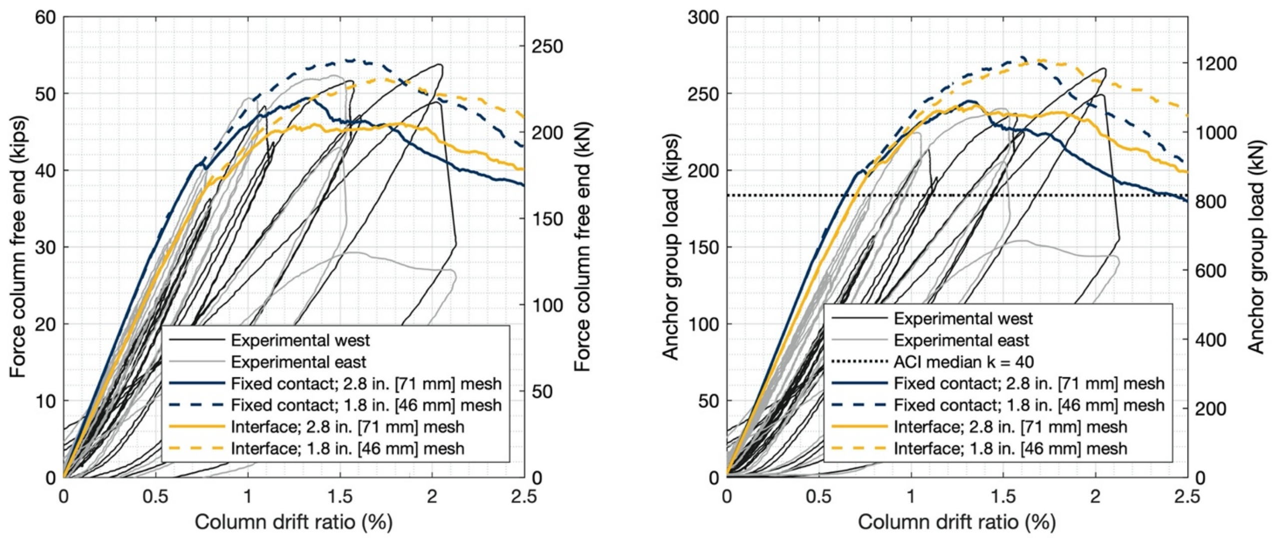

Fig. 10 – Force versus drift ratio graphs varying the base plate - concrete interface. a) load on column free end and b) anchor group load

5. Conclusions

A full-scale test specimen of an interior (not close to the foundation edges) steel-column-to-concrete-foundation connection with cast-in-place headed anchors was designed, built, and tested under incremental quasi-static cyclic loading. To isolate the effect of moment transfer, no axial load was applied to the column. The hierarchy of various failure modes was investigated.

The test specimen failed in a concrete breakout mechanism. No evidence of horizontal-joint-shear failure or strut-and-tie type failure was observed. Breakout failure does not seem to be precluded by arranging the anchors such that $z/h_{ef} = 1.3 \leq 1.4$, as suggested in the commentary of ACI 318-14 section R25.4.4.2c.

The breakout equations, from ACI 318-14 Chap. 17, describe the strength of the observed breakout failures in a satisfactory manner. The addition of the bending compressive force factor (Ψ_M) reduces conservatism. This factor is not included in ACI 318-14, but a similar version can be found in Eurocode 2 - Part 4 [15]. The breakout cones are observed to be asymmetric with a much steeper slope towards the interior of the joint. The steeper slope within the joint likely occurs because flexural compression on the bearing plate impedes the formation of a full breakout cone.

The horizontal-joint-shear strength calculated in accordance with ACI 352R-02 exceeded the breakout strength observed in the test by a wide margin, which likely explains why this failure mode was not observed. It is conceivable that a connection could be configured such that the beam-column joint strength might limit the peak strength.

The strut-and-tie model proposed underestimates the strength of the connection by a large margin and serves only as a lower bound solution for the connection. The behavior of anchors depends largely on the tensile properties of concrete, which the strut-and-tie method ignores. It is possible that an improved strut-and-tie behavior could be achieved if the anchor heads extended past the bottom reinforcing bars, thereby providing a more direct load path, but this option was not tested. The slab would have to be thickened in this zone to accommodate the deeper anchors, which would complicate construction of the connection.

FE models were calibrated with experimental data and tested for sensitivity. These models produced not only reasonable load-displacement graphs, but realistic crack patterns consistent with the observed concrete breakout failure mode. The calibrated models may be used for future parametric studies.

6. Acknowledgements

The authors wish to express their gratitude and sincere appreciation to the ACI Foundation Concrete Research Council, the AISC, and the HILTI Corporation for financing this and other on-going research projects relating to concrete anchorage. A special thanks to Ron Klemencic chairman and C.E.O. of Magnusson Klemencic Associates for material donations. The involvement of the following individuals greatly improved the quality of this investigation: Rafael Sabelli (director of seismic design at Walter P Moore), James Malley (senior principal of Degenkolb Engineers), John Silva (senior director of codes and standards at HILTI), and Roberto Piccinin (group manager code development and research at HILTI).

7. References

[1] ACI Committee 318, 2014, "Building Code Requirements for Structural Concrete (ACI 318-14) and Commentary (ACI 318R-14)," American Concrete Institute, Farmington Hills, MI, 519 pp.

[2] Fuchs, W., Eligehausen, R., and Breen, J., 1995, "Concrete Capacity Design (CCD) Approach for Fastening to Concrete," ACI Structural Journal, V. 92, No. 1, Jan.-Feb., 73-94 pp.

[3] Herzog, M., 2015, "Beitrag zur Vereinheitlichung der Bemessung im Stahlbetonbau und in der Befestigungstechnik (Contribution to the standardization of design in reinforced concrete construction and fastening technology)," Stuttgart, Germany: Institut für Werkstoffe im Bauwesen der Universität Stuttgart, 457 pp.

[4] Mahrenholtz, C., Akguzel, U., Eligehausen, R., and Pampanin, S., 2014, "New Design Methodology for Seismic Column-to- Foundation Anchorage Connections," ACI Structural Journal, V. 111, No. 5, Sep.-Oct., 1179-1189 pp.

[5] Joint ACI-ASCE Committee 352, 2002, "Recommendations for Design of Beam-Column Connections in Monolithic Reinforced Concrete Structures (ACI 352R-02)," American Concrete Institute, Farmington Hills, MI, 37 pp.

[6] Worsfold, B. and Moehle, J., 2019, "Laboratory Tests of Column-Foundation Moment Transfer Connections with Headed Anchors," Pacific Earthquake Engineering Research (PEER) Center, University of California, Berkeley, UCB/SEMM-2019/01, 171 pp.

[7] AISC, 2006, "Design Guide 1: Base Plate and Anchor Rod Design".

[8] Cervenka, J., Cervenka, V., 2020. ATENA Success Stories. Retrieved from cervenka.cz/projects/success-stories/

[9] Cervenka J, Papanikolaou V .K. Three dimensional combined fracture-plastic material model for concrete. Int. J. Plast. 2008;24:2192–220. doi:10.1016/j.ijplas. 2008.01.004.

[10] Bazant, Z.P., Oh, B.H., 1983. Crack band theory for fracture of concrete. Materials and Structures, RILEM 16 (3), 155–177.

[11] Hordijk, D.A. Local approach to fatigue of concrete. PhD Thesis, Delft University of Technology, 1991.The Netherlands.

[12] Cervenka, J., Cervenka, V., Laserna S., On finite element modeling of compressive failure in brittle materials, Computational Modeling of Concrete Structures. Bicanic et al.(Eds),Euro-C 2014, St. Anton, Austria, Tazlor & Francis Group, London, ISBN 978-1-138-00145-9, pp.273-281.

[13] Cervenka, V., Cervenka, J., Pulk, R., Sajdlova, T., 2016, "Prediction of Shear Failure of Large Beam Based on Fracture Mechanics", Proceedings 9th International Conference on Fracture Mechanics of Concrete and Concrete Structures, 8 pp.

[14] Piccinin, R., Ballarini, R., Cattaneo, S., 2012, "Pullout Capacity of Headed Anchors in Prestressed Concrete", Journal of Engineering Mechanics, ASCE, Vol. 138, No. 7.

[15] European Committee for Standardization, 2018, EN 1992-4:2018, "Design of concrete structures. Design of fastenings for use in concrete", Brussels, European Committee for Standardization.

